International Journal of Research in Engineering, Science and Management
Volume-3, Issue-8, August-2020
journals.resaim.com/ijresm | ISSN (Online): 2581-5792 | RESAIM Publishers

An Analog/Digital Controller for LED Drivers

Jaber Hasan*
Ph.D., Department of Electrical Engineering, University of Arkansas, Fayetteville, U.S.A.
*Corresponding author: j2009g@gmail.com

***Abstract*: A two-loop control scheme for LED drivers is proposed. The analog controller provides the output voltage regulation to the switch mode power converter while the digital controller injects a control signal to affect a change for the analog controller to implement an efficient constant current load. The proposed analog and digital control scheme is implemented for a two-string LED driver. The driver increases its efficiency by maintaining a minimum drive voltage across parallel-connected multiple LED strings to maintain the LED string current constant. Phase shifted PWM dimming (PSPWM) is implemented in order to reduce load current variations, improve EMI, and increase system efficiency. A mathematical model for merging the analog and digital controllers is implemented. The proposed LED driver was simulated using MATLAB SIMULINK and experimentally verified using a two-string LED load with three white LEDs in each string.**

***Keywords*: Analog controller, Digital controller, LED driver, PSPWM, SMPC.**

1. Introduction

The advancement of LED technology has led to introduction of LEDs in applications such as in liquid crystal displays (LCDs) backlight, streetlights, signage, and general-purpose lighting due to LEDs having longer lifetime, being environmentally friendly, and high efficacy [1]-[10]. LEDs are driven by constant current dc source, as their brightness is a function of the current flowing through them [1], [2], [4], [5]. In many applications, many LEDs are connected in parallel strings such as in LCD backlight applications. The drawback of connecting LEDs in parallel is the current sharing problem between the strings leading to lower lifetime for the LEDs.

There exists several ways of driving LEDs connected in parallel [1], [2], [7], [8], [11], [12], [16]. The simplest approach is to have individual drivers for each string in parallel. But these approaches require individual drivers for each LED string. Hence, it is not cost effective for drivers where large numbers of LED strings are required such as in LCD backlight or in general-purpose lighting applications.

For LED drivers driving multiple LED strings in parallel, a current controller is required for each string for maintaining the current in the string and the drive voltage is provided by the driver which is typically a switch-mode power converter (SMPC) rather than a linear regulator. In the implementation shown in Fig. 1, the drive voltage of the driver is set at its maximum by the feedback voltage in order to maintain all the current controllers in each string in regulation. In this driver, the efficiency can be maximized by selecting matched forward voltage LEDs which will lead to the added cost of the driver [1], [2].

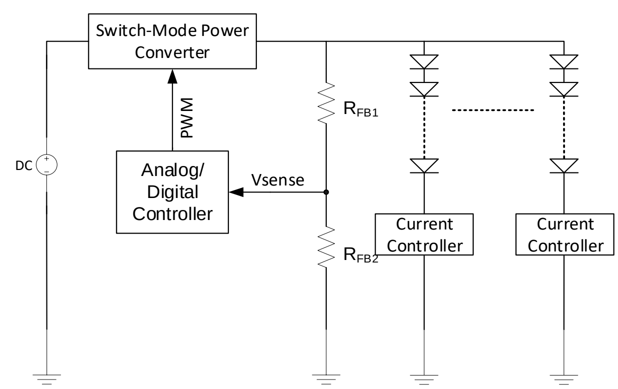

Fig. 1. A LED driver with SMPC using individual current controllers

In order to increase the efficiency at the LED load, the voltage drops across the current controllers have to be at its minimum. Approaches to increase the efficiency at the LED load, using a single analog or digital controller in the driver are proposed in [1], [2], [7], [8], [11], [16]. A different approach to driving LEDs is shown in Fig. 2 and proposed in [4], [5] for general-purpose lighting application for a single string LED load, which uses both an analog and digital controller to generate the PWM signal for the MOSFET of the switch-mode power converter. In this implementation, the digital controller produces the error signal for the analog controller. However, due to the advancement of digital controller technology, the function of the controller's in [4], [5] can be combined using a single digital controller.

In this paper, a unique two-loop control scheme for LED driver is proposed. An analog controller provides the output voltage regulation to the switch-mode power converter while the digital controller injects a control signal to affect a change for the analog controller in order to implement an efficient constant current load. A new LED driver for driving two parallel-connected strings of white LEDs and offers the maximum efficiency at the LED load is introduced based on this control scheme and is shown in Fig. 3.

In this control scheme, any off-the-shelf switch mode power converter topology such as buck or flyback converter can be used as the switch mode power converter for the LED driver.

International Journal of Research in Engineering, Science and Management
Volume-3, Issue-8, August-2020
journals.resaim.com/ijresm | ISSN (Online): 2581-5792 | RESAIM Publishers

The switch mode power converter with its analog controller forms the first loop (shown as LOOP1 in Fig. 3) and it provides the worst-case drive voltage leading to unwanted power losses in the current controllers leading to lower efficiency in the LED load. The digital controller, which forms the second loop (shown as LOOP 2 in Fig. 3), is added to lower the output voltage of the converter to its minimum value for the required load current to increase efficiency at the LED load. At startup, the converter with its analog controller works independently of the digital controller to provide the worst-case drive voltage to the parallel-connected LED load for the desired current. After the worst-case drive voltage has stabilized, the second loop injects a control signal at the feedback resistive divider node of the analog controller, leading to an increase in feedback voltage of the analog controller. In this way, the analog controller reduces the duty cycle of the PWM signal to the MOSFETs of the switch-mode power converter. This leads to a corresponding reduction of the output voltage of the converter, and thus, increases the efficiency at the LED load. Additionally, since the converter maintains regulation of the drive voltage for the LED load using only its analog controller, the system has an excellent line regulation since any changes in the input voltage are automatically adjusted by the analog loop without involving the digital controller. Additionally, the efficiency is maximized using a PSPWM dimming scheme to sequentially dim the LED strings and eliminate huge load current variations. This reduces EMI and improves system efficiency. Both mathematical models and simulation results of the proposed system will be provided in the following sections. Finally, an experimental prototype was developed to prove the concept.

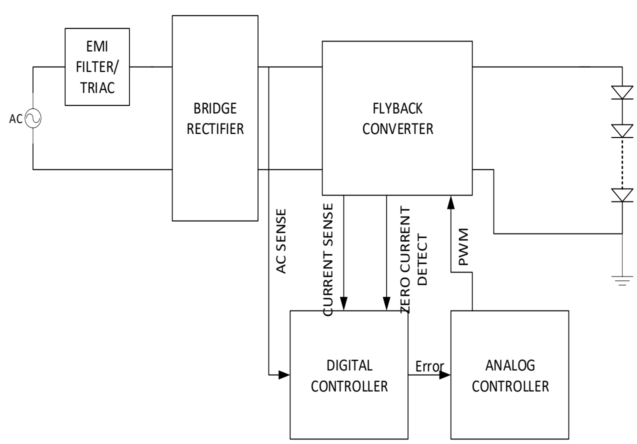

Fig. 2. A LED-driver with both analog and digital controller as implemented in [4], [5]

2. Circuit Description

The detail circuit schematic of the proposed LED-driver for driving LEDs for backlight applications is shown in Fig. 4, consisting of a dc/dc step down converter, and two strings of white LEDs array. Current is maintained in the LED strings by its corresponding current controller which senses the voltage across the sensing resistor and compares it with the reference voltage of the error amplifier. Current controllers are controlled by PSPWM signal in order to change the LED string currents. The converter provides the necessary drive voltage to the LED strings at the desired LED string current. In order to operate with minimum MOSFET drain voltage of the current controller in each string for the set LED string current, a comparator is used to compare the inverting and non-inverting voltages of the error amplifiers of the current controllers.

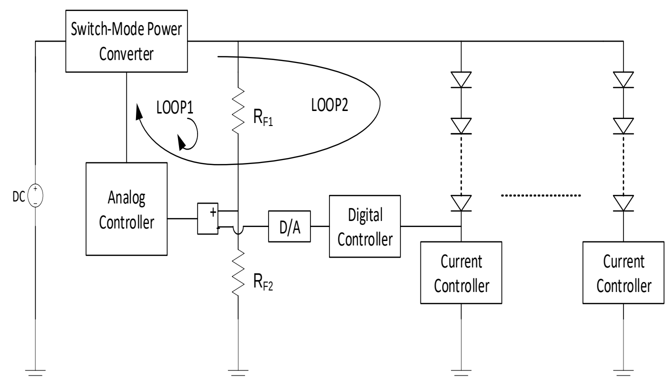

Fig. 3. Simplified circuit schematic of proposed LED-driver

The analog controller is implemented using a Texas Instruments' TL494 PWM controller to generate the drive voltage for the LED strings. The digital controller is implemented using a PIC18F4431 microcontroller which senses the output of the comparators, drain, and PWM signal of the error amplifiers of the current controller to achieve a minimum drive voltage for the LED strings at the desired load current. In order to operate with a minimum MOSFET drain voltage of the current controller in each string for the set string current, the digital controller has two different modes of operation: efficiency optimization and operation modes. These two modes of operation are very similar, but not identical to those in [7], [8]. The digital controller enables the analog controller to adjust the minimum drive voltage. The efficiency optimization routine involves finding the minimum drain voltages of the MOSFETs of the current controllers to maintain the desired LED string currents. Fig. 5 shows the flowchart for this mode. The operation mode generates an error voltage by comparing the minimum drain voltage with a reference voltage. This error voltage is used by a proportional-integral-derivative (PID) controller to generate the necessary PWM signal, first filtered by a low-pass active gain filter, and then fed to a feedback node of the analog controller. Fig. 6 shows the flowchart for this mode.

A. *Efficiency Optimization Mode*

1) Initially, the converter supplies a non-optimized drive voltage to the LED strings operating at the desired load current. This voltage is sufficient to maintain the MOSFETs of the current controllers in saturation, leading to unwanted power losses in the current controllers.

International Journal of Research in Engineering, Science and Management
Volume-3, Issue-8, August-2020
journals.resaim.com/ijresm | ISSN (Online): 2581-5792 | RESAIM Publishers

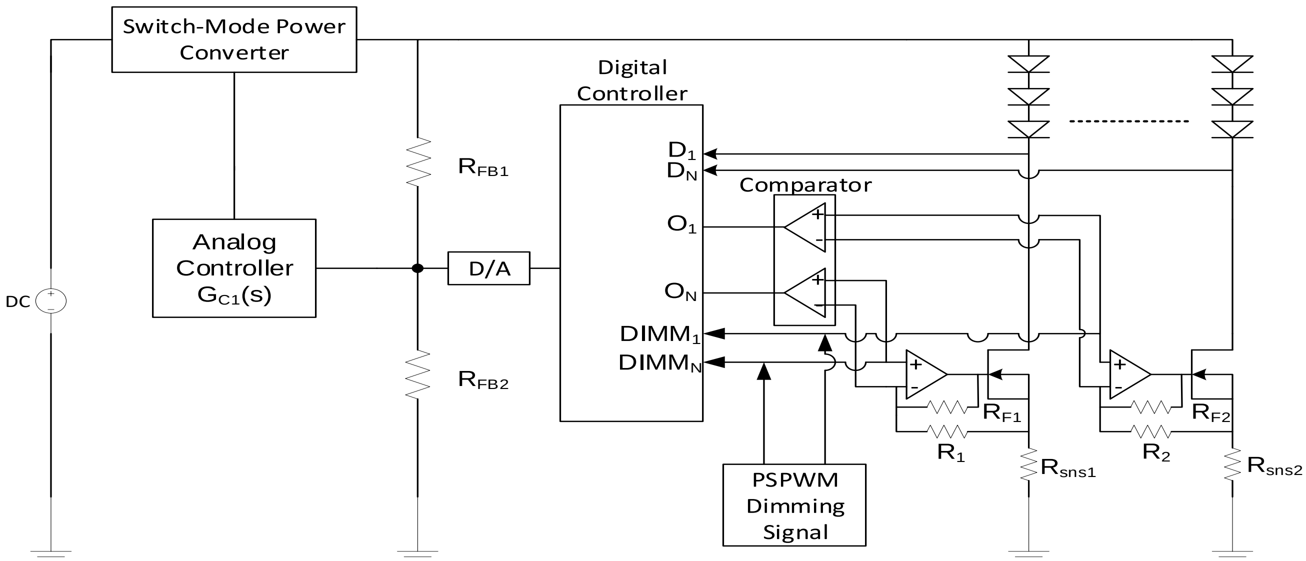

Fig. 4. Detail circuit schematic of proposed LED-driver

2) After the worst-case output voltage of the switching converter stabilizes, the digital controller determines the maximum value from the sensed output of the comparators which compares the inverting and non-inverting voltages of the error amplifiers of each current controller in the LED strings.
3) This maximum voltage is compared against a threshold value. This value is necessary to maintain the desired LED string currents at the minimum drain voltages of the current controllers in each string. If the sensed maximum comparators output voltage is below this threshold value, the duty cycle of the PWM signal for the second controller is increased. The digital controller repeats this step until the maximum sensed comparators output voltage is greater than the threshold value, indicating that one or both of the LED strings are no longer in regulation.

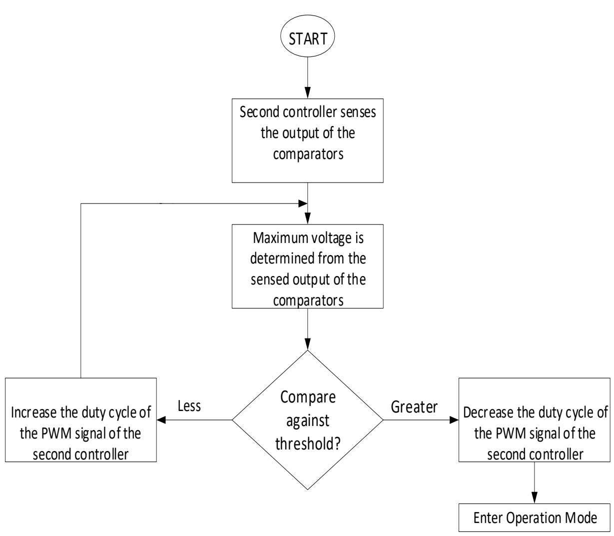

Fig. 5. Flowchart of efficiency optimization mode

4) At this time, the duty cycle of the PWM signal of the second controller is reduced to achieve the minimum drive voltage. Then, the digital controller enters the operation mode.

B. Operation Mode

1) The microcontroller senses the drain voltages of the two-current controlled MOSFETs and finds its minimum value and stores this as the reference voltage at the beginning of operation mode at the set current level. The PWM signals of the error amplifiers of the current controllers are also sensed during this mode, and then stored at the beginning of this mode.
2) This reference voltage is compared against the sensed minimum drain voltage of the MOSFETs to generate the error voltage. A PID controller processes this error voltage to generate the desired PWM signal for the digital controller, first filtered into a dc value by a low-pass active filter, and then, fed into the feedback point.
3) If the sensed PWM signal of the error amplifiers of the current controller changes, then the microcontroller exits the operation mode and returns to the efficiency optimization mode to find the minimum drain voltage of the MOSFETs of the current controllers at the new LED string current setting.

3. Controller Design

The controller for the second loop is designed in digital domain because the control algorithm can be easily implemented using a single microprocessor or digital-signal-processor (DSP), offers flexibility as the controller can be easily changed by the software, and the digital controllers are not susceptible to temperature and aging of circuit components [13]. The block diagram of the entire system is shown in Fig. 7. In the block diagram, $G_{C1}(s)$ and $G_{C2}(z)$ are the analog and digital controller of the system, respectively, $G_P(s)$ is the plant

International Journal of Research in Engineering, Science and Management
Volume-3, Issue-8, August-2020
journals.resaim.com/ijresm | ISSN (Online): 2581-5792 | RESAIM Publishers

or the switch-mode power converter, H_1 and H_2 are the feedback gains of the analog and digital controller, respectively, $1/V_M$ is the PWM modulator gain, $G_{ADC}(z)$ and $G_{DAC}(s)$ are the transfer function of the analog-to-digital converter and digital-to-analog converter, respectively, and $V_{REF1}(s)$ and $V_{REF2}(z)$ are the references of the analog and digital controller, respectively.

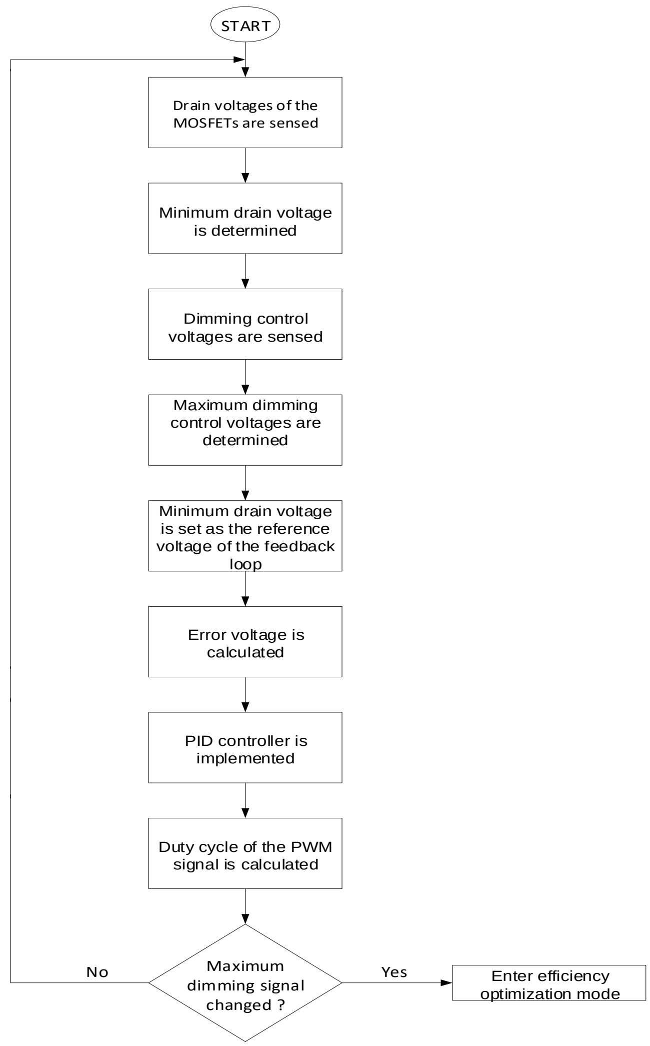

Fig. 6. Flowchart of operation mode

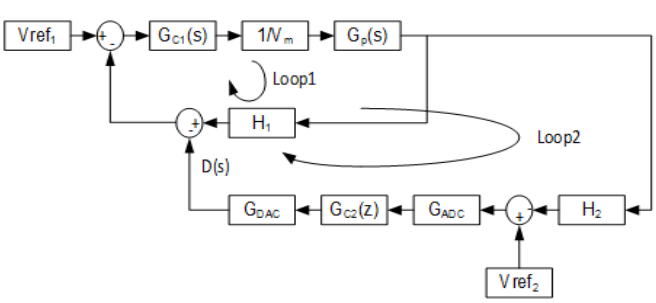

Fig. 7. Block diagram of the complete system

In order to find the relationship of the output voltage with respect to $V_{REF1}(s)$ and $V_{REF2}(z)$, a superposition theory was implemented on the block diagram in Fig. 7. Ideally, superposition cannot be implemented in a non-linear switch-mode power converter system. However, since the converter with its analog controller (loop 1) is operating at 200 kHz and the LED current dimming frequency is between 100-400 Hz, the driver output changes only when the signal from the digital controller (loop 2) changes. Additionally, due to the slow change nature of the LED forward voltage, the superposition theory can be implemented in this system [8].

The signal coming from the second loop is defined as D(s) in the block diagram. So, when $V_{REF2}(z)$ is set to zero, thus, D(s) is also zero, the block diagram reduces to the one shown in Fig. 8. From Fig. 8, we can deduce,

$$V_{O1}(s)=\frac{G_{C1}(s)*G_P(s)*\frac{1}{V_M}}{1+\frac{H_1*G_{C1}(s)*G_P(s)}{V_M}}V_{REF1}(s) \quad (1)$$

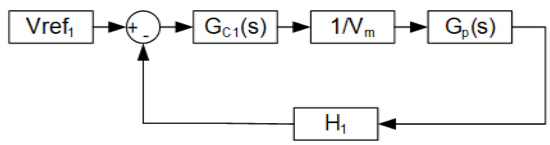

Fig. 8. Block diagram with $V_{REF2}(z)$ set to zero

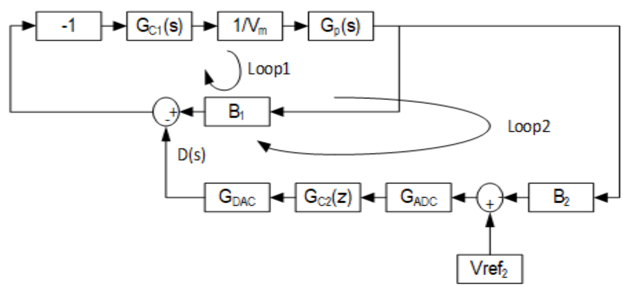

Fig. 9. Block diagram with $V_{REF1}(s)$ set to zero.

Next, to find the relationship of the $Vo_2(s)$ with respect to $V_{REF2}(z)$, $V_{REF1}(s)$ is set to zero and the block diagram reduces to as shown in Fig. 9. From Fig. 9, we can deduce,

$$V_{O2}(s)=\frac{G_{C1}(s)*G_P(s)*\frac{1}{V_M}*G_{C2}(z)*G_{ADC}(z)*G_{DAC}(s)}{1+\frac{H_1*H_2*G_{C1}(s)*G_P(s)*G_{C2}(z)*G_{ADC}(z)*G_{DAC}(s)}{V_M}}V_{REF2}(z) \quad (2)$$

Therefore, Vo(s) is total effect of both $V_{O1}(s)$ and $V_{O2}(s)$. So we can deduce from (1) and (2) that,

$$V_O(s)=\frac{G_{C1}(s)*G_P(s)*\frac{1}{V_M}}{1+\frac{H_1*G_{C1}(s)*G_P(s)}{V_M}}V_{REF1}(s)+$$

$$\frac{G_{C1}(s)*G_P(s)*\frac{1}{V_M}*G_{C2}(z)*G_{ADC}(z)*G_{DAC}(s)}{1+\frac{H_1*H_2*G_{C1}(s)*G_P(s)*G_{C2}(z)*G_{ADC}(z)*G_{DAC}(s)}{V_M}}V_{REF2}(z) \quad (3)$$

International Journal of Research in Engineering, Science and Management
Volume-3, Issue-8, August-2020
journals.resaim.com/ijresm | ISSN (Online): 2581-5792 | RESAIM Publishers

4. System Considerations

The design aspects of the proposed LED driver are discussed in detail below for driving a two LED strings in parallel for an LCD backlight application.

A. Design of Power Stage

In this implementation, a closed loop dc-dc buck converter is designed using a Texas Instruments' TL494 PWM controller. The input voltage available was 24V and the worst-case output voltage was 13V at the set load current of 400mA. The switching frequency of the converter was chosen to be 200 kHz and a phase margin of 35° was chosen to ensure a stable loop response.

The buck converter was designed to satisfy the allowed ripple magnitudes of the inductor current and capacitor voltage and to operate it in continuous conduction mode. The inductor current ripple is defined as,

$$\Delta I_L = \frac{V_S D(1-D)}{f_S L} \quad (4)$$

where V_S is the nominal input voltage, D is the duty cycle, f_S is the switching frequency, and L is the inductor value [14]. Thus, from (4) the inductor value was found to be 150µH.

Similarly, the capacitor ripple voltage is,

$$\Delta v_C = \frac{V_S D(1-D)}{8 f_S{}^2 LC} \quad (5)$$

which yield a capacitance of 100µF [14].

Fig. 8 shows the simplified block diagram of voltage-mode controlled power circuit. The control to output transfer function of the plant ($G_P(s)$) for the block diagram shown in Fig. 8 is,

$$\frac{\hat{v}_O}{\hat{d}} = \frac{V_O}{D}\left(\frac{1+sR_C C}{1+s\left(R_C C+\left[R//R_L\right]C+\dfrac{L}{R+R_L}\right)+s^2 LC\left(\dfrac{R+R_C}{R+R_L}\right)}\right) \quad (6)$$

In the above equation (6), R_C and R_L are the parasitic resistance associated with the capacitance and inductance of the power circuit. The load resistance R is assumed to be resistive. The effective load resistance is the parallel combination of two LED strings in parallel with three LEDs in series for each string. Since the typical forward voltage of the chosen LEDs are 3.5 V, therefore,

$$R_{EQU} = \frac{V_{FWD}}{I_{LED}} = \frac{10.5}{200*10^{-3}} = 52.5\Omega \quad (7)$$

$$R_{SINGLE\_STRING} = R_{EQU} + R_{DS} + R_{SENSE} = 52.5 + 1.8 + 0.6 = 54.9\Omega \quad (8)$$

$$R_{OUT} = 27.45\Omega \quad (9)$$

From (6) and (8), the transfer function for a voltage-mode controlled buck converter becomes,

$$Gp(s) = \frac{2.4*10^{-5}s+24}{7.495*10^{-9}s^2+6.343*10^{-6}s+1} \quad (10)$$

Using MATLAB, a PID compensator is designed for the power circuit. The closed loop bode plot of the compensated power circuit is shown in Fig. 10. As can be seen, the crossover frequency and phase margin are 32 kHz and 34°, respectively. The corresponding transfer function of the controller is,

$$G_{C1}(s) = 3.257*10^6\left(\frac{s^2+7.8*10^3 s+6.6*10^6}{s^3+1.957*10^5 s^2+9.57*10^9 s}\right) \quad (11)$$

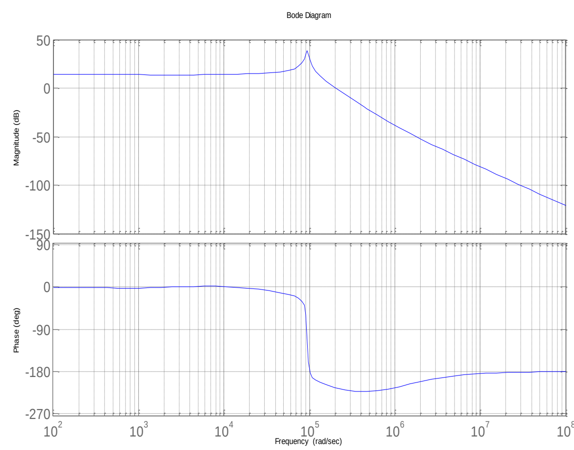

Fig. 10. Bode plot of the compensated power circuit

B. Dimming Circuit

The brightness of each string in the multi-loop driver can be individually dimmed using either an analog dimming or a conventional pulse-width-modulation (PWM) dimming.

Analog dimming is easier to implement but suffers from linear change in brightness and chromaticity at the lower current levels due to I-V characteristics of a diode [15], [16], [18]. Hence, in mixed mode dimming, analog dimming is implemented for up to 7% of the nominal LED string current, and then changes to PWM dimming for linear change in brightness [15]. Typically, the frequency of the PWM dimming is about 100-400 Hz for LCD backlight applications.

However, the major disadvantages of the conventional PWM dimming is its higher ripple output voltage and EMI issues due to sudden changes in input-output current if all the LEDs are turned on and off at the same time [1], [11], [16], [17]. Thus, phase-shifted (PS) PWM dimming as described in [1], [11], [16], [17] is implemented in this LED driver system. In PSPWM dimming, the LED string draws current sequentially rather than simultaneously as in conventional PWM dimming. There are several advantages of PSPWM dimming over conventional PWM dimming such as the lower output voltage ripple and the peak to peak LED current is smaller than the conventional PWM dimming [1], [11], [16], [17].

Phase delay in PSPWM dimming is calculated using,

$$\theta = \frac{360^o * (k-1)}{N} \quad (11)$$

where k is the selected LED string and N is the total number of LED strings in parallel in the driver [17]. Therefore, the delay between the dimming signal at LED string 1 and LED string 2 is 180° for this implementation.

C. Design of Controller for the second feedback loop

The second controller is first designed in analog domain and then converted into the digital domain. Fig. 11 shows the block diagram of the whole system with the second loop in s domain. Using MATLAB, the overall closed loop Bode plot of the LED driver given by equation (3) is shown in Fig. 12 when the G_{C2} is set to 1. As shown, the crossover frequency is found to be 30 kHz and the phase at the crossover frequency is 33°, implying the driver system is stable.

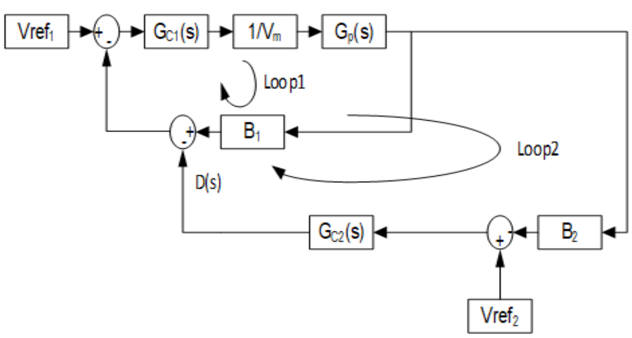

Fig. 11. Block diagram of the complete system with the second loop in s domain

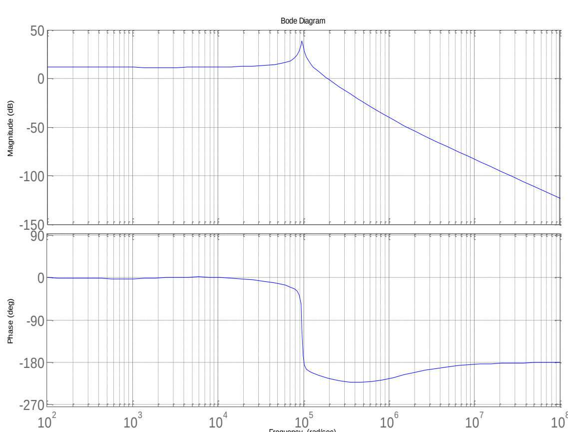

Fig. 12. Bode plot of the LED driver with respect to both V_{REF1} and V_{REF2} when G_{C2} is equal to 1

Using MATLAB, a suitable PID controller was designed as described by equation (12). The overall closed loop Bode plot of the LED driver is shown in Fig. 13 with the $G_{C2}(s)$ as described by equation (12). As shown, the crossover frequency is found to be 28 kHz and the phase at the crossover frequency is 32°, indicating a stable driver system.

$$G_{C2}(s) = 2 + \frac{1*10^4}{s} + 1.1881*10^{-4}s \quad (12)$$

Since the controller G_{C2} will be implemented using the PIC18F4431 microcontroller, equation (12) needs to be converted into its digital domain using a 'matched pole-zero' method with a sampling period of 20μs. Therefore,

$$G_{C2}(z) = \frac{7.012z^2 - 11.82z + 5.008}{z-1} \quad (13)$$

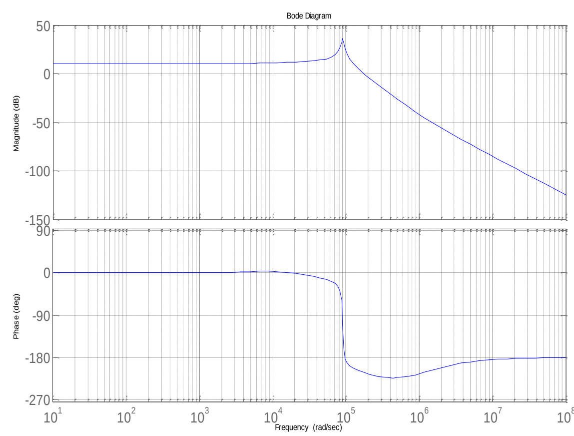

Fig. 13. Bode plot of the LED driver with respect to both V_{REF1} and V_{REF2} when $G_{C2}(s)$ is equal to the designed PID controller in (12)

D. Merging digital to analog controller

The digital controller shown in (13) has to be transformed into s domain according to [19] which uses a multi-rate simulation technique described in [20]. It is known that if an s domain term is sampled it produces a loss of information [19]. According to [19], a term in z domain can be transformed into s domain assuming the damped natural frequency in each conjugate pole pairs of the controller is sampled at a period T according to [19],

$$\omega_I < \frac{\Pi}{T}, \forall i \quad (14)$$

Thus, every pole of the z domain can be easily transformed into s domain using the relation in [19],

$$p_I = \frac{1}{T}[\ln p_I + i\beta_I] \quad (15)$$

Then, $G_{C2}(z) = \Im[G_{C2}(s)]$ by incorporating partial fraction expansion, and then, finding the poles in the s domain using (15) as shown in [19]. Therefore, the s domain equivalent controller for (13) is,

$$G_{C2}(s) = 9.3 + \frac{1*10^4}{s} \tag{16}$$

Using MATLAB, the overall closed loop Bode plot of the LED driver is shown in Fig. 14 with $G_{C2}(s)$ shown in equation (16). As shown, the crossover frequency is found to be 30 kHz and the phase at the crossover frequency is 34°, indicating a stable driver system.

5. Simulation Results

The performance of the proposed LED driver was verified using MATLAB SIMULINK. A dc-dc buck converter was designed to drive two parallel LED strings with three LEDs in series for each string. The driver without the digital loop was designed to provide the worst-case output voltage of 13V at a load current of 400mA. Usually, a lower forward voltage than the maximum forward voltage specified in the LED datasheet is required to drive the LEDs at the specified current. Thus, the output voltage of the driver should be adjusted to the minimum voltage required for the load current by adding the digital loop in order to increase the efficiency at the LED load.

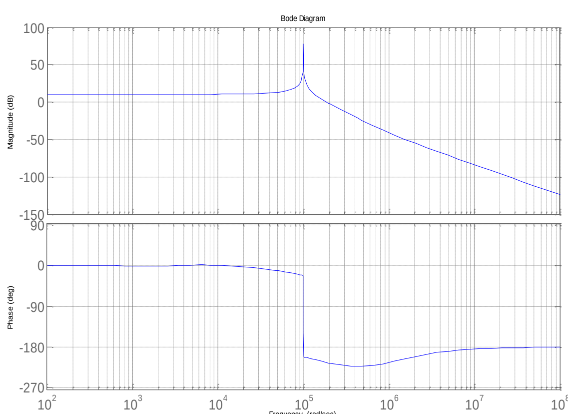

Fig. 14. Bode plot of the LED driver with respect to both V_{REF1} and V_{REF2} when $G_{C2}(s)$ is equal to the PI controller in (16)

Fig. 15(a) shows the output voltage of the driver being adjusted to its minimum value required to maintain an output load current of 400mA with the digital controller implemented as shown in (13). As shown, the output voltage changes from worst-case 13V to optimum value of 10V in about 4ms. The current drops to about 270mA momentarily but it recovers back to 400mA during this interval as shown in Fig. 15(b). Fig. 15(c) shows the control signal from the digital controller. As can be seen from Fig. 15(c), the control signal from the controller $G_{C2}(z)$ responds to changes in the feedback voltage of the analog controller to maintain the minimum voltage across the LED strings. This leads to an improvement in efficiency of the LED load.

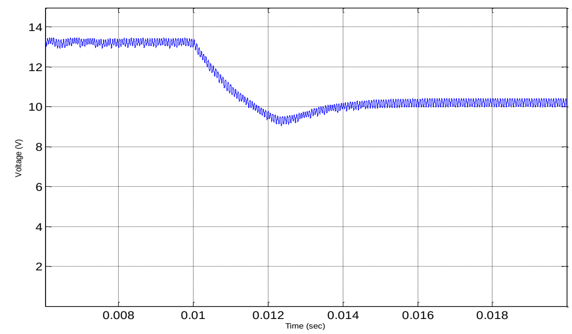

(a)

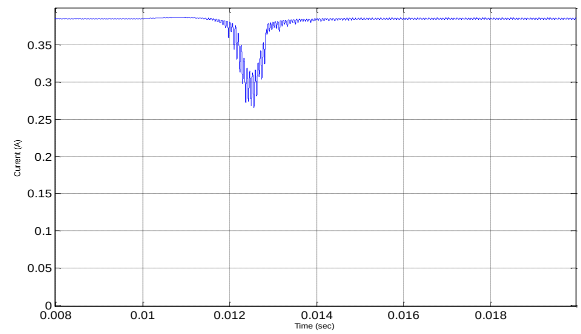

(b)

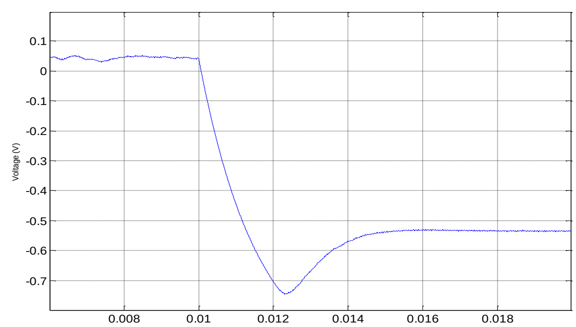

(c)

Fig. 15. (a) Output Voltage of the driver (b) Output Current of the driver and (c) Output Voltage from the second controller

6. Experimental Results

The performance of the proposed LED driver was experimentally verified using a dc-dc buck converter operating from an input voltage of 24 V at a switching frequency of 200 kHz. The LED load consisted of two parallel strings of three series-connected white LEDs, each having a worst-case forward voltage of 4V. Initially, the driver provides an output voltage of 13 V at a current of 400mA. The digital controller determines the minimum output voltage necessary to maintain a 200mA of current in each of the two LED strings by injecting a control voltage at the feedback node of the analog controller after the initial worst-case drive voltage has stabilized. Fig. 16 shows the waveforms of the driver. As can be seen, the driver achieves a minimum drive voltage needed to maintain the LED string current. The upper waveform (Channel 1) is the output voltage of the driver, the second waveform (Channel 2) shows the output of the digital controller, the third waveform (Channel 3) shows duration of the efficiency optimization-mode, and the lower waveform (Channel 4) is the output current of the driver. It can be seen from Fig. 16 that the output voltage adjusts to 10.3 V from the initial 13V to maintain the desired 200mA of LED current. The signal output of the digital controller is zero initially when the output voltage is at its maximum value of 13V. During the optimization mode of the digital controller, the driver output voltage adjusts its output signal fed into the feedback node of the analog controller until it reaches 10.3V which is needed to maintain the 400mA load current in the LED strings. The efficiency of the LED driver is defined as,

$$Efficiency = \frac{P_{LED}}{P_{STRING}} \times 100 \tag{17}$$

Thus, the efficiency of the LED driver at the initial output voltage of 13 V is 70% while the efficiency at 10.3 V is 90%. This is an improvement of a 20% increase in efficiency. This clearly demonstrates the functionality of the two loop LED driver in improving the efficiency.

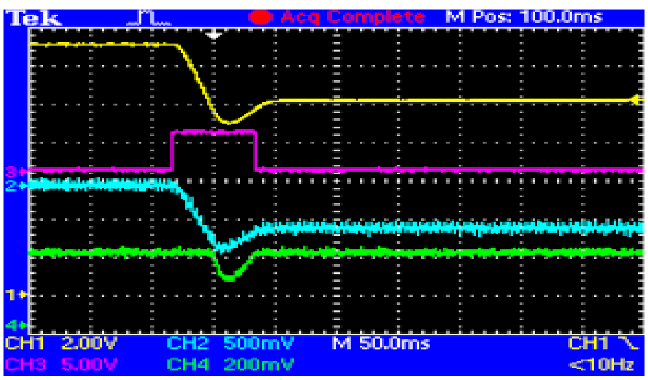

Fig. 16. Measured output voltage, duration of efficiency optimization mode, output of the second controller and output current of the driver during adjustment of output drive voltage of the LED driver

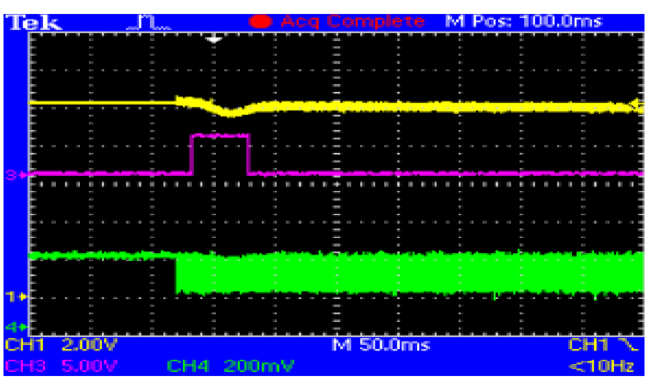

Fig. 17. Measured transient response from 100% to 80% duty cycle PWM signal

In this proposed LED driver, each string of LEDs receives its PSPWM dimming signal as described earlier. The load transients of the LED strings from 100% duty cycle PWM signal to 80% duty cycle PWM signal are shown in Fig. 17. The upper waveform (Channel 1) is the output voltage of the driver, the middle waveform (Channel 3) shows the duration of the efficiency optimization-mode, and the lower waveform (Channel 4) is the output current of the driver. It can be observed from Fig. 17 that in order to improve the efficiency, the optimization-mode is enabled in order to reduce the output voltage of the LED driver to its minimum value required to maintain the desired LED string current.

Additionally, the advantage of using PSPWM is verfied in Fig. 18 in order to demonstrate the self-adjustment of the output voltage of the driver to improve efficiency. The upper waveform (Channel 1) is the output voltage of the driver, the middle waveform (Channel 4) is the output current of the driver, and the remaining two waveforms (Channel 2 and Channel 3) are the PSPWM signal of the current controllers of the LED strings. As can be seen from the Fig. 18, that the output voltage of the driver is adjusted in a step fashion leading to minimum drop across the current controllers in the LED strings [21].

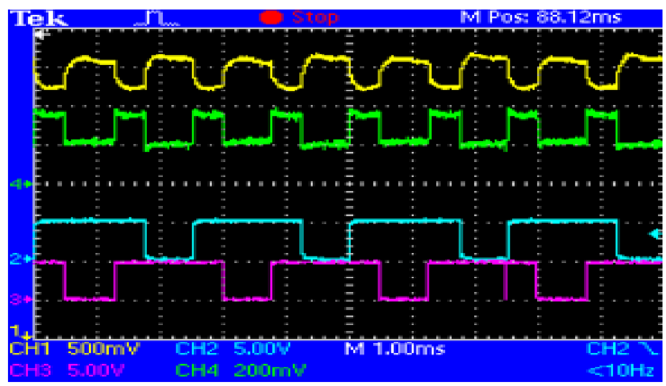

Fig. 18. Measured output voltage, output current and the PSPWM signals of the current controllers of the LED strings

7. Conclusion

A LED driver for driving multiple strings of LEDs in backlight application for display panels using a two-loop control scheme was designed and implemented in this paper. The efficiency of the proposed driver was maximized by adjusting the output voltage of the driver to a minimum value necessary to drive the LED load at the desired string current. A PSPWM dimming was implemented to alleviate the problems associated with PWM and analog dimming of LEDs, leading to better overall efficiency of the driver. In this implementation, the drive voltage of the LEDs and the current of the LEDs were controlled separately to improve stability [22]. The two-loop controlled LED driver was experimentally verified to achieve a 20% improvement in efficiency for a parallel-connected LED load with three series-connected LEDs in each string at a load current of 400mA.

References

[1] Yuequan Hu, and Milan M. Jovanovic, "LED Driver with Self-Adaptive Drive Voltage," *IEEE Transactions on Power Electronics*, vol. 23, no. 6, pp. 3116-3125, Nov 2008.

[2] Yuequan Hu, and M. M. Jovanovic, "A Novel LED Driver with Adaptive Drive Voltage," in *Proc. IEEE Appl. Power Electron. Conf. (APEC), 2008*, pp. 565-571.

[3] Hao Wu, Siu-Chung Wong, Chi K. Tse, and Qianhong Chen, "A PFC Single-Coupled-Inductor Multiple-Output LED Driver Without Electrolytic Capacitor," *IEEE Transactions on Power Electronics*, vol. 34, no. 2, pp. 1709-1725, Feb. 2019.

[4] J. Zhang, H. Zeng, and T. Jiang, "A primary-side control scheme for high-power-factor LED driver with TRIAC dimming capability", *IEEE Transactions on Power Electronics*, vol. 27, no. 11, pp. 4619-4629, Nov 2012.

[5] L. Xu, H. Zeng, J. Zhang, and Z. Qian, "A primary side controlled WLED driver compatible with TRIAC dimmer*", in Proc. IEEE Appl. Power Electron. Conf. (APEC)*, 2011, pp. 699-704.

[6] Zheng Dong, Chi K. Tse, and S.Y. Ron Hui, "Circuit Theoretic Considerations of LED Driving: Voltage-Source Versus Current-Source Driving", *IEEE Transactions on Power Electronics*, vol. 34, no. 5, pp. 4689-4702, May. 2019.

[7] J. Hasan, and S. S. Ang, "A high-efficiency digitally controlled RGB-driver for LED pixels," *IEEE Transactions on Industry Applications*, vol. 47, no. 6, pp. 2422-2429, Nov-Dec 2011.

[8] J. Hasan, Do Hung Nguyen, and S. S. Ang, "A RGB-driver for LED display panels," in *Proc. IEEE Appl. Power Electron. Conf. (APEC), 2010*, pp. 750-754.

[9] Cassio Gobbato, Samuel V. Kohler, Ithalo H. de Souza, Gustavo W Denardin, and Juliano de Pelegrini Lopes, "Integrated Topology of DC-DC Converter for LED Street Lighting System Based on Modular Drivers", *IEEE Transactions on Industry Applications*, vol. 54, no. 4, pp. 3881-3889, Aug. 2018.

[10] Wu Chen, and S. Y. R. Hui, "A dimmable light-emitting diode (LED) driver with mag-amp postregulators for multistring applications," *IEEE Transactions on Power Electronics*, vol. 26, no. 6, pp. 1714-1722, June 2011.

[11] M. Doshi and R. Zane, "Digital architecture for driving large LED arrays with dynamic bus voltage regulation and phase shifted PWM," in *Proc. IEEE Appl. Power Electron. Conf. (APEC)*, 2007, pp. 287-293.

[12] Cikai Ye, Pritam Das, and Sanjib K. Sahoo, "Peak Current Control of Multichannel LED Driver with Selective Dimming", *IEEE Transactions on Industrial Electronics*, vol. 66, no. 5, pp. 3446-3457, May. 2019.

[13] Queenie Le, Deyu Chen, Daryl Cher, David Ho, Iulian Mirea, Rex Wong, and Ricky Setiawan, "A digitally controlled embedded SMPS with 2.3V to 5.5V input voltage for mobile SoCs", *International Symposium on Integrated Circuits, 2016*, pp. 1-4.

[14] S. S. Ang and Alejandro Oliva, *Power-Switching Converters*, 2nd ed., Boca Raton, FL: CRC Press, 2005.

[15] Jeff Falin. (2010, January). How to Dim a WLED Backlight Driver. *The Mag. Of Solid-State Lighting.*
Available: http//www.ledjoutnal.com/eprints/TI_Jan10.html

[16] Pang-Jung Liu, Yu-Chi Hsu, and Shang-Ru Hsu, "Drain-Voltage Balance and Phase-Shifted PWM Control Schemes for High-Efficiency Parallel-String Dimmable LED Drivers", *IEEE Transactions on Industrial Electronics*, vol. 65, no. 8, pp. 6168-6176, Aug. 2018.

[17] Yu-Kang Lo, Kuan-Hung Wu, Kai-Jun Pai, and Huang-Jen Chiu, "Design and Implementation of RGB LED Drivers for LCD Backlight Modules", *IEEE Transactions on Industrial Electronics*, vol. 56, no. 12, pp. 4862-4871, Dec 2009.

[18] K. I. Hwu, W. C. Tu, and C. Y. Lai, "Light-emitting diode driver with low-frequency ripple suppressed and dimming efficiency improved," IET Power Electron, vol. 7, no.1, pp. 105–113, Jun. 2014.

[19] V. Feliu, "A transformation algorithm for estimating system Laplace transform from sampled data," *IEEE Transactions on Systems, Man and Cybernetics*, vol. SMC-16, No. 1, pp. 168-173, Feb 1986.

[20] R. Aracil, A. Jimenez, and V. Feliu, "Multirate sampling technique in digital control systems simulation," *IEEE Transactions on Systems, Man and Cybernetics*, vol. SMC-14, no. 5, pp. 776-780, Sept. 1984.

[21] Yuequan Hu, M. M. Jovanovic, and C. Weng, "Driver that efficiently regulates current in a plurality of LED strings," U.S. Patent 2009/0187925 A1, Jul. 23, 2009.

[22] Do Hung Nguyen, J. Hasan, and S. S. Ang, "A built-in self-test high-current LED driver," *in Proc. IEEE 8th Int. Conf. on ASIC (ASICON)*, 2009, pp. 340-343.